Journal of Physics: Conference Series **3143** (2025) 012083 doi:10.1088/1742-6596/3143/1/012083

A modeling approach for sizing on-site hydrogen refueling stations

D. Lanni[1*], G. Di Cicco[1], G. Erme[2], A. Perna[1], A. Agresta[3], M. Della Pietra[3], and V. Cigolotti[4]

[1] Department of Civil and Mechanical Engineering, University of Cassino and Southern Lazio, Cassino, Italy
[2] Department of Electrical and Information Engineering, University of Cassino and Southern Lazio, Cassino, Italy
[3] DTE-PCU-SPCT, ENEA R. C. Casaccia, Rome, Italy
[4] TERIN-PSU-ABI, ENEA Portici, Portici, Italy

[*]E-mail: davide.lanni@unicas.it

Abstract. On-site hydrogen refueling stations (HRSs) play a crucial role in promoting the development of sustainable mobility, as they provide enhanced flexibility and scalability compared to centralized hydrogen production systems. These stations can be established in various locations, including remote areas and densely populated urban areas, without the need for a complex transportation network. Furthermore, on-site HRSs allow for meeting local demand, tailoring the hydrogen production, making these stations particularly suitable for facilitating the gradual adoption and exploitation of fuel cell-based vehicles. In this work, a modeling approach for sizing a small on-site HRS is presented. This kind of station consists of two main sections: the hydrogen production system and the refueling line. In particular, in the analyzed configurations, hydrogen is produced on-site by means of electrolysis units powered by photovoltaic or wind plants. The refueling line is based on a three-cascade storage system. Dynamic models able to forecast the hydrogen demand and to size both the hydrogen production section and the refueling line have been developed. Considering a specific case study, the numerical approach is used to size a small on-site grid-connected HRS.

1. Introduction

In recent years, issues such as climate change, the exhaustion of fossil fuels, and the increasing demand for energy have highlighted the urgent need for clean fuel alternatives [1]. In particular, according to IEA, total CO_2 emissions associated with energy reached an unprecedented 37.8 gigatons in 2024, suggesting an increasing growth driven significantly by the transportation sector [2]. In this context, green hydrogen, produced from renewable energy sources such as solar and wind, is viewed as the ideal long-term carbon-neutral alternative to hydrocarbons [3], [4]. However, to promote its use in the transport sector, it is crucial to address the development of the required infrastructure, especially hydrogen refueling stations (HRSs). In particular, refueling stations with on-site hydrogen production are playing an essential part in the shift towards sustainable mobility, providing more flexibility and scalability compared to centralized hydrogen production systems [5]. In fact, these stations can be established in various locations, including remote areas and densely populated urban centers, thereby removing the

Content from this work may be used under the terms of the Creative Commons Attribution 4.0 licence. Any further distribution of this work must maintain attribution to the author(s) and the title of the work, journal citation and DOI.
Published under licence by IOP Publishing Ltd

need for a complex transportation network [5] and effectively matching local fuel demand by customizing hydrogen production, thus promoting the integration of fuel cell vehicles in the existing fleet [6]. In recent years, many studies have been devoted to investigating the techno-economic feasibility of on-site hydrogen refueling stations.

Di Micco et al. [7] carried out the sizing of an on-site hydrogen refueling station based on alkaline electrolysis and powered by a photovoltaic (PV) plant. To meet a daily hydrogen production target of 450 kg stored at a maximum pressure of 900 bar, a 2.1 MW electrolyzer and an 8 MW PV system are required. The system also includes a 3.5 MWh lithium-ion battery for excess electricity storage, with grid connectivity for surplus energy export. A study by Mahmood et al. [8] assessed a PV-powered hydrogen refueling station able to produce 160.68 kg of green hydrogen per day. Different configurations of the HRS were examined, and a sizing methodology was developed, according to which a 2.8 MWp solar power plant alongside a 0.515 MW PEM electrolyzer was necessary. The study by Lanni et al. [9] evaluates the techno-economic feasibility of a grid-connected hydrogen production plant with a capacity of 1,000 kg/day of hydrogen, for an on-site HRS considering various electrolysis technologies, two different power sources (PV and wind turbines), and three potential installation sites. Furthermore, two different management strategies are proposed: operating the electrolysis unit at full load for 8,000 hours, and running it only when the renewable energy source (RES) is active. A numerical model in Matlab was used for the techno-economic evaluation, revealing that the PV-alkaline-based configurations were the most convenient from an economic point of view. Ren et al. [10] created an extensive dynamic model for a hydrogen refueling station using MATLAB, which covers the entire refueling process, from the station tanks to the vehicle, including compressor dynamics. This validated model is employed to evaluate the impact of critical parameters (such as hydrogen storage pressure and temperature, target state of charge of the vehicle’s tank) on the refueling performance.

Although there is a growing number of studies focusing on the feasibility of on-site HRSs, the majority of them use simplified assumptions, or, alternatively, despite incorporating the dynamic approach in modeling, they do not address the integration of hydrogen production under varying demand conditions. This work addresses this gap by developing a dynamic modeling approach able to size both the production and refueling sections of an on-site grid-connected HRS.

2. Methodology

This section presents the proposed methodological approach for the sizing of an on-site HRS. The proposed methodology (whose workflow is depicted in Figure 1) is articulated in four main steps:

1. First of all, a semi-randomized algorithm is developed in order to generate realistic hourly hydrogen demand profiles based on the characterization of the vehicles’ fleet;
2. Secondly, a refueling line, based on a three-stage cascade storage system to optimize compression and distribution consumptions, is modelled;
3. Then, the hydrogen production section is sized according to the hourly hydrogen demand profile and storage requirements;
4. Finally, the modeling approach is applied to a case study, whose technical assessment is carried out through the evaluation of the system components’ sizes and mass and energy balances.

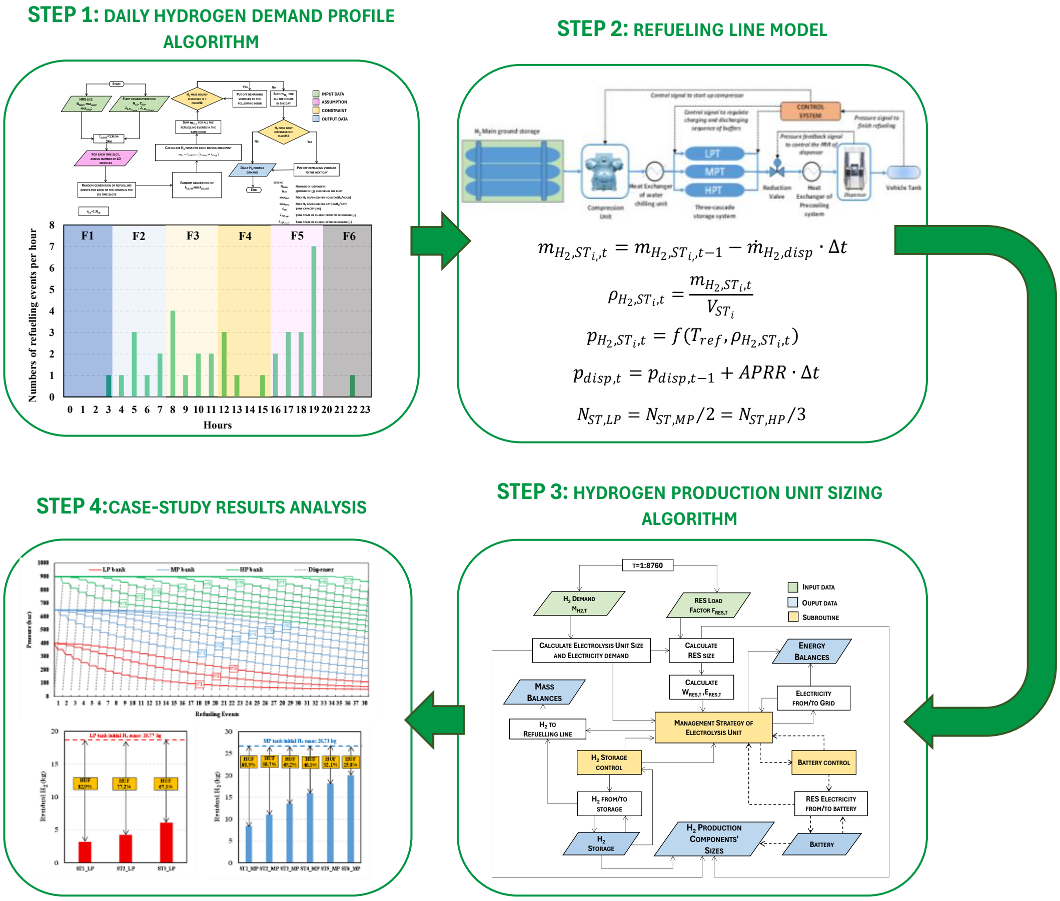

Figure 1. Workflow of the proposed methodology for the modeling process of an on-site HRS

Figure 2 shows a schematic depiction of the on-site HRS examined in this research, and designed to serve a local fleet of light-duty vehicles. The HRS comprises two main subsystems: the hydrogen production section (HPS) and the refueling line (RL).

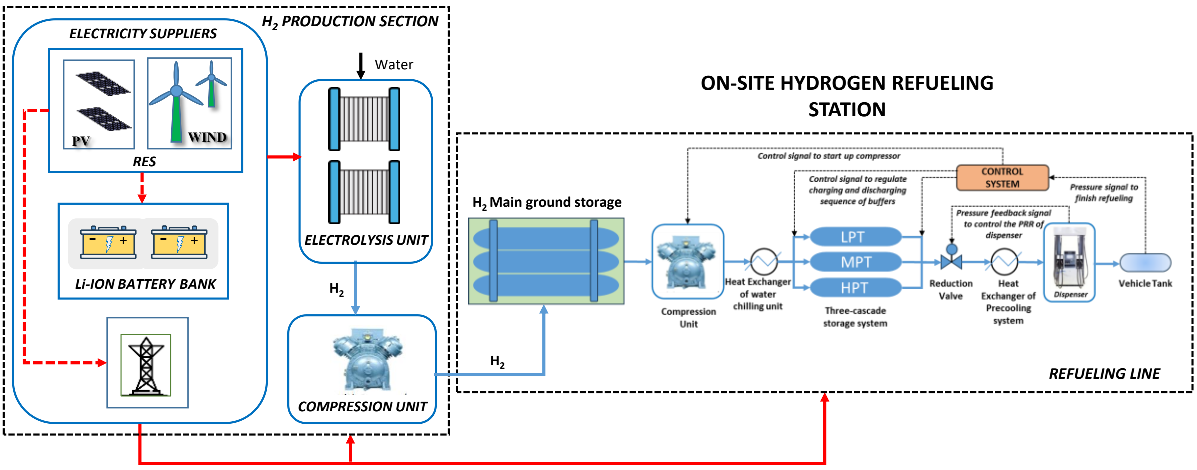

Figure 2. Schematic representation of the on-site HRS.

Journal of Physics: Conference Series **3143** (2025) 012083 doi:10.1088/1742-6596/3143/1/012083

The HPS includes a water electrolyzer and a compression and buffer storage unit (200 bar) powered by a grid-connected Renewable Energy System (RES), which is also equipped with a battery pack to balance power supply fluctuations. Electricity from the RES is used to operate the electrolyzer directly; any surplus is first stored in the battery and eventually delivered to the grid, while energy shortages are compensated using battery-stored energy before drawing from the grid.

The RL, instead, is based on a cascade storage system, which consists of three banks: low-pressure (LP) bank, medium-pressure (MP) bank, and high-pressure (HP) bank. They operate at 900, 650, and 400 bar, respectively. Each bank is composed of multiple storage tanks (STs) of the same volume. During refueling operations, hydrogen is delivered starting from the low-pressure vessel and then progressively from the medium- and high-pressure ones. This approach enables a significant reduction (30–40%) in the power demand of the compression unit compared to single-stage storage systems [11], [12]. For the analyzed small HRS, a single dispenser is considered.

2.1 Daily hydrogen demand profile algorithm

The daily hydrogen demand profile is crucial not only to design the on-site HRS, since it influences the station's configuration and component selection [13], but also to evaluate the refueling line's electrical consumption. Despite this, many feasibility studies only consider the total daily demand, without accounting for how hourly variations impact the operation and dimensioning of system elements [14], [15]. To address this gap, an algorithm has been developed, whose workflow is shown in Figure 3.

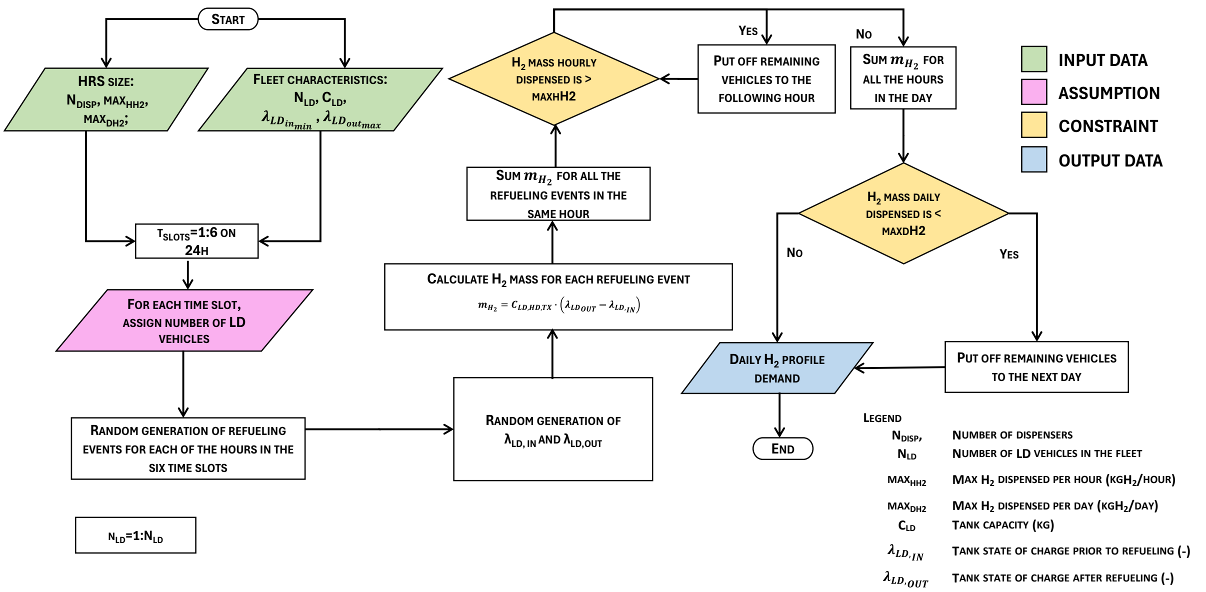

Figure 3. Workflow of the daily hydrogen profile algorithm.

The algorithm generates random refueling events over 24 hours based on the station and fleet's characteristics, calculating the hydrogen dispensed for each event and producing a daily demand curve with an hourly resolution. The main input data includes:

– HRS size and characteristics, including the station's size (in this case, small), number of dispensers, maximum daily refueling events, hourly dispensing capacity, and total daily dispensing limit;

– Fleet characteristics, which in this case study are made up of a single vehicle type, which is the Light Duty Vehicle (LD) for private and goods transport, with up to 9 seats;

To model typical daily refueling patterns, the 24-hour period is divided into six time slots. Each time slot is assigned a percentage of the total LD vehicles expected to refuel during that day. Once the time slots and vehicle shares have been established (based on the premise that the highest volume of vehicles will arrive at the station during the time slots just before and after typical office hours), the hourly distribution of refueling events is randomly generated within a single time slot. This provides the number of LD vehicles refueled in each hour. The resulting hourly distribution is then used to build matrices representing the initial and final state of charge (SOC) of each vehicle's tank. These SOC values are assigned randomly, but always within a predefined input range. The hydrogen dispensed per refueling event is calculated as:

$$m_{H_2,LD} = C_{LD} \cdot \left(\lambda_{LD,out} - \lambda_{LD,in}\right) \tag{1}$$

Where C_{LD} (kg) is the tank capacity of LD vehicles, while $\lambda_{LD,in}$ $\lambda_{LD,out}$ are the initial and final SOC values, respectively.

The sum of hydrogen dispensed for all events in a specific hour gives the hourly hydrogen demand. A constraint within the algorithm ensures that the maximum allowable hydrogen flow rate per hour is not exceeded. If this limit is surpassed, vehicles are either queued to the next hour or marked as not refueled, in the case of the last hour of the day. Figure 3 shows the workflow of the daily hydrogen demand profile algorithm.

The characteristics of a small HRS and of the vehicles' fleet are shown in Table 1, while Table 2 reports data regarding the time slots and the assigned percentages of the total refueling events for a specific day.

Table 1. Small HRS parameters [16].

Parameter	Unit	Value
Dispensers' number	-	1
Maximum waiting time between two successive refueling events	min	5
Maximum hourly hydrogen flow	kg/h	33.6
Maximum daily hydrogen flow	kg/day	200
Type of refueled vehicles	-	LD
Maximum number of refueling events per day	-	38
Tank's capacity	kg	5.1
$\lambda_{LD,in}/\lambda_{LD,out}$	%	20-60/70-98

Table 2. Distribution of time slots and percentage of refueling events.

Slot	Hour range	Percentage of refueling events
F1	0:00-3:59	$X_{F1,LD}$=5%
F2	4:00-7:59	$X_{F2,LD}$=30%
F3	8:00-11:59	$X_{F3,LD}$=20%
F4	12:00-15:59	$X_{F4,LD}$=5%
F5	16:00-19:59	$X_{F5,LD}$=35%
F6	20:00-23:59	$X_{F6,LD}$=5%

To ensure a conservative approach to the sizing of the refueling station, the algorithm can predict a Worst-Case Scenario (WCS), in which the hydrogen dispensed over 24 hours is at the maximum required level. In fact, in this scenario, the SOC of every incoming vehicle's tank is assumed to be 10%, while the filling state of every outgoing vehicle's tank is assumed to be 100%. This indicates that, for every refueling event, the dispensed flow rate remains constant and equal to the maximum possible. This methodology has been chosen to perform the sizing of the refueling station.

2.2 Refueling Line modeling

The refueling line (Figure 4) has been modelled considering its two main subsystems: the three-cascade storage system and the dispenser [17].

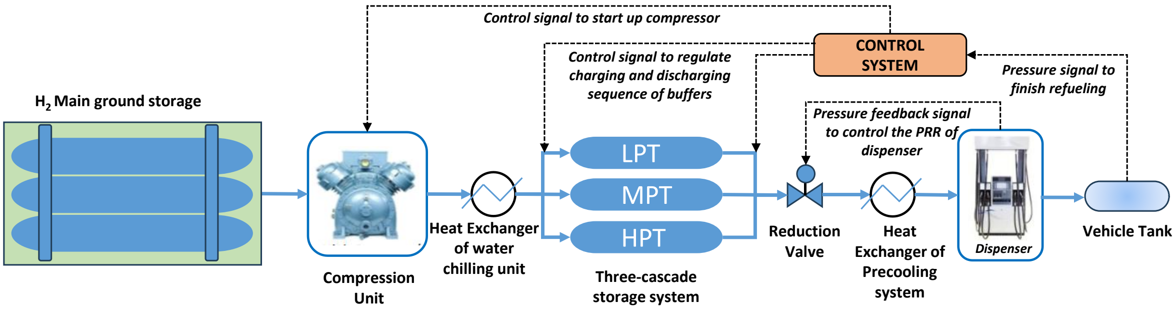

Figure 4. Schematic representation of a refueling line based on a three-cascade storage system.

The refueling process has been schematized by means of a mass balance between the two subsystems. The real gas equation of state of hydrogen has been used, exploiting the NIST database [18]. The set of equations (2)-(5) is solved for each ST of the cascade system:

$$m_{H_2,ST_i,t} = m_{H_2,ST_i,t-1} - \dot{m}_{H_2,disp} \cdot \Delta t \tag{2}$$

$$\rho_{H_2,ST_i,t} = \frac{m_{H_2,ST_i,t}}{V_{ST_i}} \tag{3}$$

$$p_{H_2,ST_i,t} = f(T_{ref}, \rho_{H_2,ST_i,t}) \tag{4}$$

$$p_{disp,t} = p_{disp,t-1} + APRR \cdot \Delta t \tag{5}$$

where $m_{H_2,ST_i,t}$ is the mass of H_2 in the *i-th* storage tank at time t, $\dot{m}_{H_2,disp}$ is the average hydrogen mass flow rate delivered to the dispenser, $\rho_{H_2,SU_i,t}$ and $p_{H_2,SU_i,t}$ are the density and the pressure, respectively, in each ST at time t, V_{ST_i} is the volume of the *i-th* ST, T_{ref} is a reference temperature considered equal to 15°C, $p_{disp,t}$ is the pressure at the dispenser at time t, $APRR$ is the average pressure ramp rate during the refueling process, and Δt is the considered time step equal to 1 s. As the pressure at the dispenser increases and approaches the decreasing pressure of the storage tank, the refueling process shifts to the next storage tank, which can either be from the same bank or from another unit that operates at a higher pressure. This operation continues until the target pressure at the dispenser is achieved, and the process is reiterated until all refueling tasks are completed. In particular, for each refueling event, the first storage tank of the HRS that operates in the cascade system is always the one with the lowest pressure. The target pressure at the dispenser must not exceed the 125% of the Nominal Working Pressure (NWP), i.e. 700 bar for light-duty vehicles [17].

The number of STs (N_{ST}) of the three banks is chosen by taking into account the following relationship [17]:

$$N_{ST,LP} = N_{ST,MP}/2 = N_{ST,HP}/3 \quad (6)$$

The size of the H_2 main ground storage is chosen as twice the maximum daily hydrogen demand and increased by 20%, allowing for defining a proper hourly hydrogen demand profile for the sizing of the hydrogen production section. In particular, in this study, the hourly hydrogen demand is considered constant and equal to 1/24 of the maximum daily hydrogen demand.

2.3 Hydrogen Production Section sizing

The third step of the modeling approach consists of the development of an algorithm for the sizing of the hydrogen production section, whose workflow is shown in Figure 5.

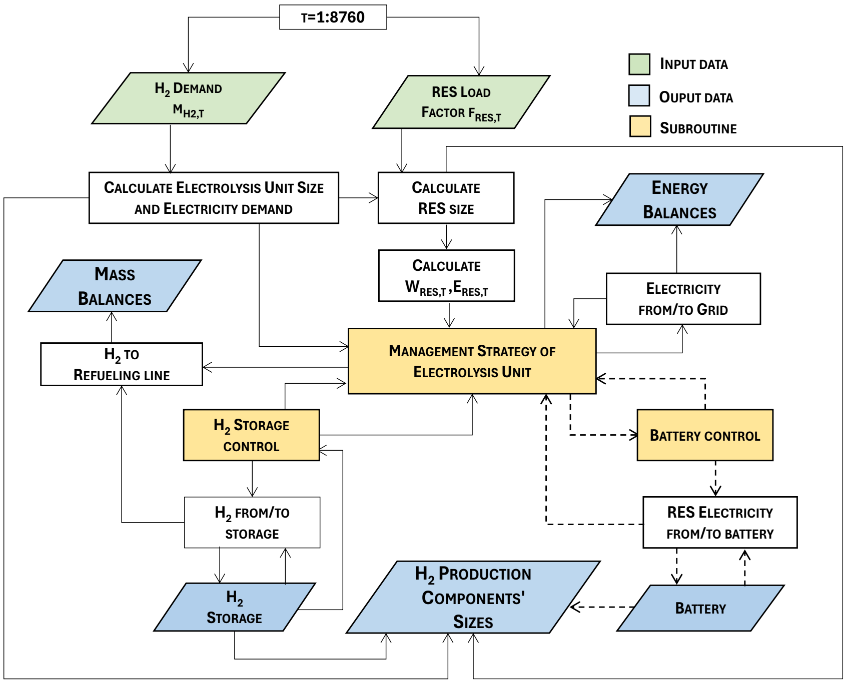

Figure 5. Workflow of the hydrogen production section sizing.

The algorithm requires three different sets of input data:

- the renewable energy potential at the installation site (expressed through the RES load factor).
- the performance characteristics of the selected RES technology;
- the hourly hydrogen demand profile ($M_{H2,t}$).

Furthermore, the algorithm is governed by two key sizing criteria:

1. the electrolysis unit is sized to meet the maximum hourly hydrogen demand;
2. the renewable energy system (RES) is sized to cover the annual electricity consumption of the electrolysis unit, of the compression units of both HPS and RL, and of the pre-cooling unit of the RL.

The algorithm carries out dynamic mass and energy balances and incorporates a priority-based energy management strategy to control power allocation: electricity from the RES is first used to supply the electrolyzer, then to charge the battery pack (if present), and finally, any surplus is exported to the grid. On the contrary, when RES output is insufficient, electricity is drawn first from the battery and then from the grid. This logic is reflected in the battery control subroutine shown in the workflow.

3. Case study

The developed numerical approach has been used to size a small on-site HRS, which uses a photovoltaic (PV) plant as RES. The plant is located in Central Italy (latitude 42.43, longitude 11.77). The selected PV system utilizes Jinko Solar's 560W monocrystalline silicon modules (44.31V@12.63A), which exhibit a 20.5% efficiency under standard test conditions (STC). The optimal inclination and azimuth angles for the photovoltaic cells were determined based on the climatic and meteorological conditions of the installation site. The capacity factor of the considered PV plant is equal to 19%. For the battery pack, the Tesla Megapack Li-ion battery, characterized by a round-trip efficiency of 88 % and a power-to-energy ratio of 741.2 kW/2964.8 kWh, has been selected [19].

The electrolysis unit, based on PEM (proton exchange membrane) technology, consists of 100 kW modules and operates at 20 bar and 55 °C [20], [21]. In the nominal operating condition, the average cell voltage and current density are 2.17 V and 2,99 A/cm^2, respectively, while the power consumption of the auxiliary is assumed to be 2.8% of the rated power [20], [21]. The nominal hydrogen output for each module is 1.68 kg/h, with a specific energy consumption equal to 59 kWh/kg (the efficiency, referred to the Low Heating Value of hydrogen, is 56.5%).

4. Results

4.1 Daily hydrogen demand profile

In this section, the results of the daily hydrogen demand profile algorithm are presented. First of all, Figure 6 shows a typical distribution of refueling events in a single day. It is worth noticing that the peak of refueling events, equal to seven, is reached at 7 p.m.

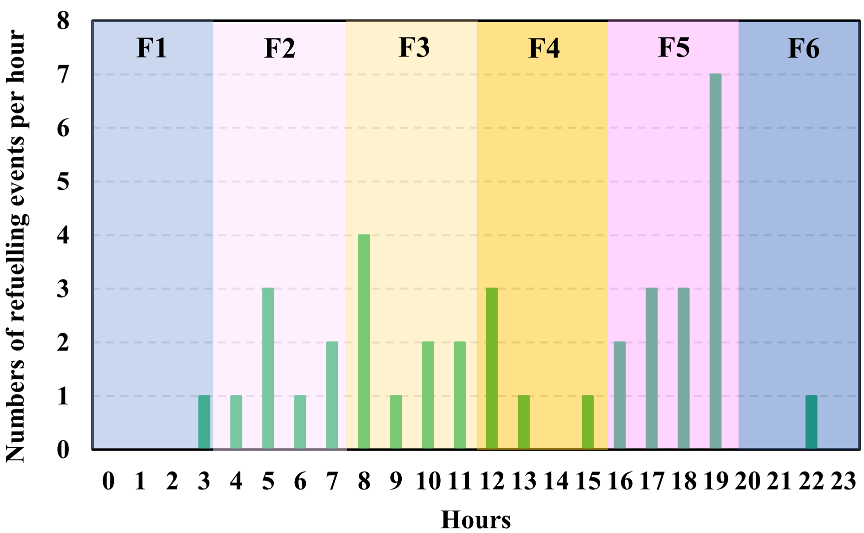

Figure 6. Distribution of refueling events in a single day.

Figure 7, instead, illustrates the two hourly profiles of hydrogen demand, one representing the typical case and the other depicting the worst-case scenario.

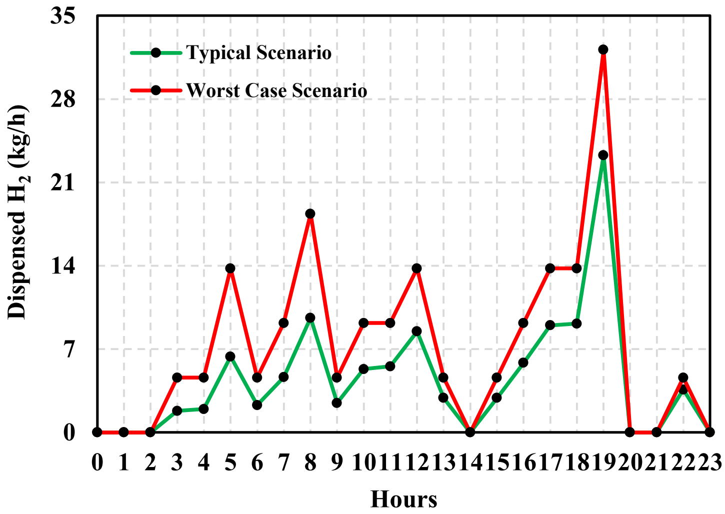

Figure 7. Hourly hydrogen demand profile in the typical scenario (green line) and in the worst-case scenario (red line).

By examining Figure 7, it is evident that, in the example provided, even in the worst-case scenario, the hourly demand always remains below the constraints imposed on the maximum deliverable flow rate (33.6 kg_{H2}/h, see Table 1), amounting to 32.1 kg_{H2}/h. The daily flow of hydrogen also adheres to the maximum allowable daily output constraint, which is set at 200 kg/day, both in the case of the typical profile (105 kg_{H2}/day) and in the worst-case scenario (174.4 kg_{H2}/day).

4.2 Refueling line

The sizing of the refueling line is carried out by exploiting the results obtained using the daily hydrogen demand profile algorithm. In particular, the RL is sized in order to allow the execution of the intended refueling events each day in succession, meaning there is no waiting period or compression phases between two successive refuelings. Consequently, the hydrogen banks of the cascade system can be refilled at the conclusion of the working day.

Since the duration of the refueling event (refueling time) is equal to 5 minutes, and by assuming an initial pressure at the dispenser of 50 bar, the $APRR$ has been set to 159 bar/min. This leads to a target pressure equal to 842.4 bar, which is lower than the considered limit value, i.e., 875 bar. The average hydrogen mass flow rate delivered to the dispenser, $\dot{m}_{H_2,disp}$, results equal to 0.918 kg/min, calculated considering the total hydrogen dispensed in a single refueling event (4.59 kg) divided by the refueling time.

The results of the sizing of the RL, obtained by applying the described methodology, are reported in Table 3.

Table 3. Refueling line sizing results.

Parameter	Unit	Value
$N_{ST,LP}$ / $N_{ST,MP}$ / $N_{ST,HP}$	-	3 / 6 / 9
V_{ST}	m^3	0.7
H_2 main ground storage size (200 bar)	kg (m^3)	418.6 (27.7)

Figure 8 shows the pressure evolution inside the STs of each bank in the worst-case scenario and considering that the 38 refueling events occur in sequence (the total time is 190 min). The dispenser pressure for each refueling event is also represented. According to the defined strategy, when the pressure at the dispenser increases and gets close to the lower pressure of the storage tank, the refueling process shifts to the next storage tank, which may be from the same bank or from a different unit that operates under a higher pressure. As an example, for the 1st refueling event, the first storage tank of the LP bank (ST1) starts the refueling process, and its pressure consequently reduces approaching the dispenser pressure. The process continues switching to the ST2 of the same bank and, following the same mode, the refueling continues first with the ST1 of the MP bank and then with the ST2 of the same bank. The refueling event is completed with the ST1 of the HP bank.

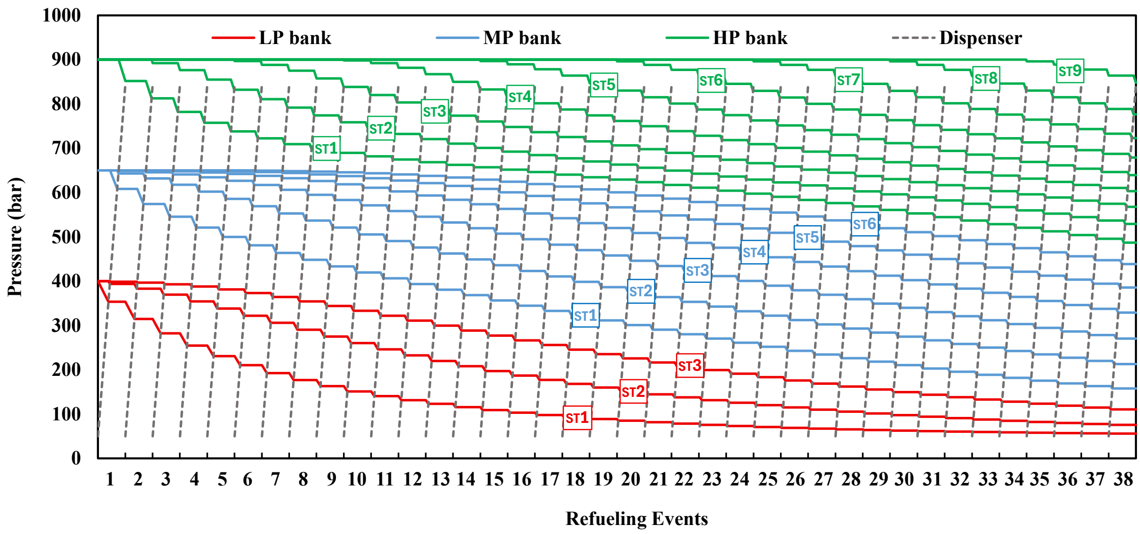

Figure 8. Pressure evolution in the three-cascade storage system for each refueling event according to the required dispenser pressure.

Figure 9 presents the residual H_2 mass in the three-cascade storage system after the 38 refueling events and the hydrogen utilization factor (HUF) for the different STs. The HUF is calculated as:

$$HUF = 1 - \frac{m_{H2,residual}}{m_{H2,initial}} \tag{7}$$

where $m_{H2,initial}$ is the initial H_2 mass in the ST, and $m_{H2,residual}$ is the residual H_2 mass at the end of the last refueling event. It is worth noting that the hydrogen utilization factor (HUF) decreases moving from the LP to the HP bank. This is in accordance with the pressure trends presented in Figure 8, taking into account that the tanks of the HP bank do not excessively reduce their pressure, delivering a lower hydrogen mass to the dispenser compared to the storage banks operating at lower pressures. Considering the three different banks of the cascade system, the HUF is equal to 75.8%, 45.6%, and 19.7% for the LP, MP, and HP banks, respectively. The hydrogen utilization factor of the entire cascade system is equal to 33.9%.

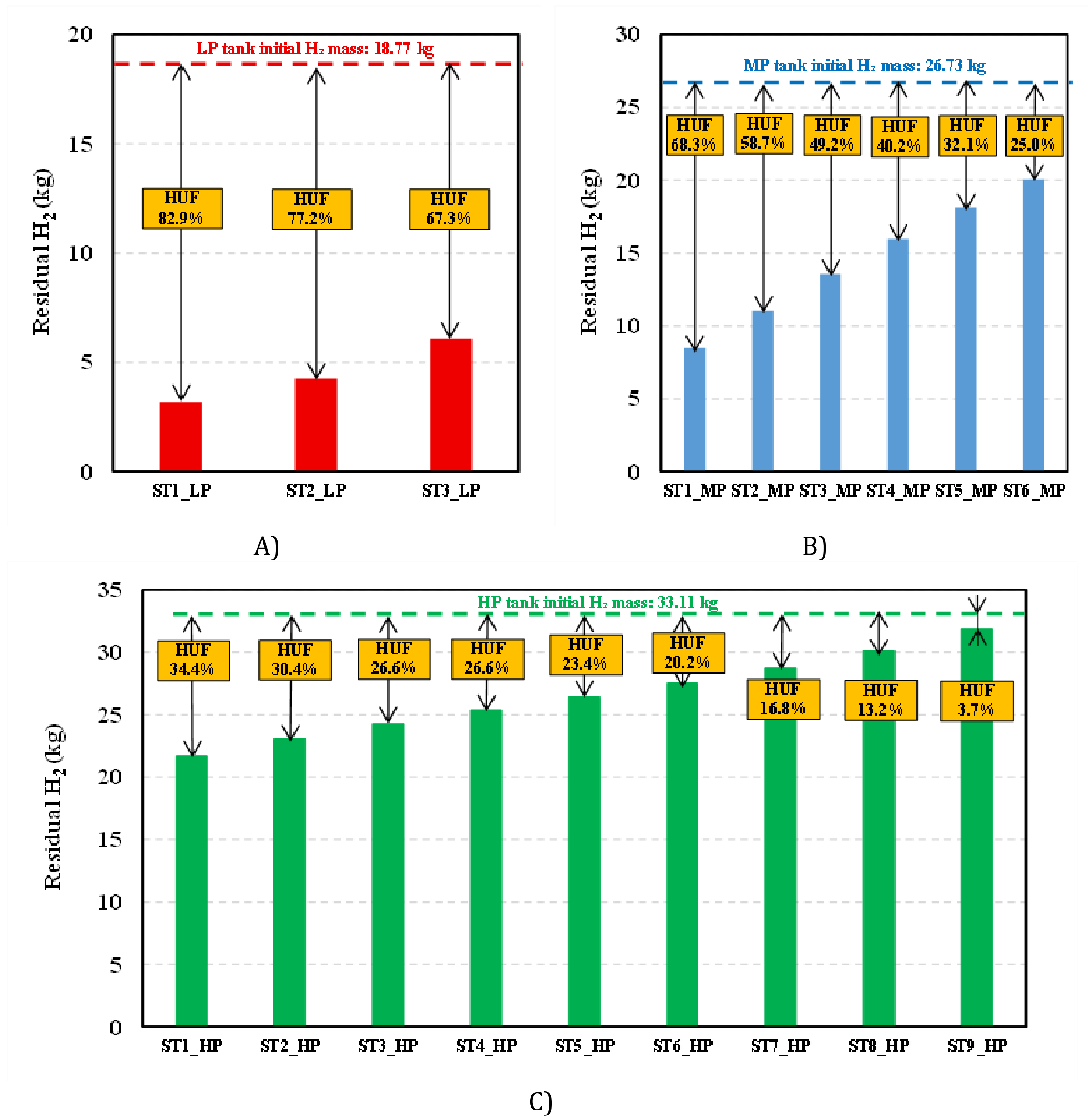

Figure 9. Residual H_2 mass for the low pressure (A), medium pressure (B), and high pressure (C) storage tanks after the 38 refueling events.

4.3 Hydrogen production section

Referring to the hydrogen production section, it has been sized according to the proposed strategy, considering a constant hourly hydrogen production equal to 7.27 kg/h (it is stored at 200 bar). Moreover, the size of the PV plant is calculated for satisfying the annual electricity required by the HRS (i.e. the annual electricity consumption of the electrolyzer, of the compression units of both HPS and RL, and of the pre-cooling unit of the RL), while the battery size is chosen in such a way the net energy stored allows powering the electrolysis unit at full load for 4h. The specific energy consumption of the RL's pre-cooling unit is assumed equal to 2.0 kWh/kg [22] while those of the refilling process of the cascade system are assumed equal to 0.9, 1.4, and 2.0 kWh/kg for the LP, MP, and HP banks, respectively. The specific consumption of the compression unit of the HPS is considered equal to 1.2 kWh/kg. The results of the sizing procedure are reported in Table 4.

Table 4. Hydrogen production section sizing results.

Parameter	Unit	Value
PV plant size	MW	2.44
Electrolysis unit size	kW	500
Compression unit size	kW	10
Battery pack size	MWh	2.3

The plant produces a total annual hydrogen amount equal to about 63.7 tons, with an annual electricity excess diverted to the grid equal to 1802.5 MWh, and integrates 1748.1 MWh of electricity from the grid over the year.

5. Conclusions

In this work, a modeling approach for sizing a small on-site HRS, designed to serve a local fleet of light-duty vehicles, is presented. Dynamic models have been developed to predict the hydrogen demand and to size both the hydrogen production section and the refueling line. The developed numerical approach has been used to size a small on-site grid-connected HRS, which uses a PV plant as RES. The main results can be summarized as:

- A worst-case scenario for the hydrogen demand profile has been identified, in which the maximum hourly demand is 32.1 kg_{H2}/h, while the daily flow of hydrogen is equal to 174.4 kg_{H2}/day;
- The three-cascade storage system of the refueling line is composed of 3 LP tanks, 6 MP tanks, and 9 HP tanks of 0.7 m^3 each. The HUF is equal to 75.8%, 45.6%, and 19.7% for the LP, MP, and HP banks, respectively, while the HUF of the entire cascade system is equal to 33.9%.
- The hydrogen production section is composed of a 2.44 MW PV plant equipped with a 2.3 MWh battery pack, a 500 kW electrolysis unit, and a 10 kW compressor unit. It produces about 63.7 tons of hydrogen per year, diverting an annual electricity excess to the grid equal to 1802.5 MWh, and integrates 1748.1 MWh of electricity from the grid over the year.

Acknoledgements

This research was funded by the European Union - NextGenerationEU from the Italian Ministry of Environment and Energy Security, POR H2 AdP MEES/ENEA with involvement of CNR and RSE, PNRR - Mission 2, Component 2, Investment 3.5 "Ricerca e sviluppo idrogeno", CUP: I83C22001170006.

References

[1] T. Nawaz Chaudhary, A. Akbar, M. Usman, M. Atif Mahmood, A. O. M. Maka, and B. Chen, "Parametric sensitivity analysis to investigate the effects of operating and design parameters on single direct methane steam reforming solid oxide fuel cell performance and thermal impacts generation," *Energy Conversion and Management: X*, vol. 18, no. December 2022, p. 100374, 2023, doi: 10.1016/j.ecmx.2023.100374.

[2] IEA, "Global Energy Review 2025," 2025.

[3] P. Marocco, M. Gandiglio, and M. Santarelli, "Optimal design of PV-based grid-connected hydrogen production systems," *Journal of Cleaner Production*, vol. 434, no. November 2023, p. 140007, 2024, doi: 10.1016/j.jclepro.2023.140007.

[4] S. Ramakrishnan, M. Delpisheh, C. Convery, D. Niblett, M. Vinothkannan, and M. Mamlouk, "Offshore green hydrogen production from wind energy: Critical review and perspective," *Renewable and Sustainable Energy Reviews*, vol. 195, no. February, p. 114320, 2024, doi: 10.1016/j.rser.2024.114320.

[5] T. L. Berg, D. Apostolou, and P. Enevoldsen, "Analysis of the wind energy market in Denmark and future interactions with an emerging hydrogen market," *International Journal of Hydrogen Energy*, vol. 46, no. 1, pp. 146–156, 2021, doi: 10.1016/j.ijhydene.2020.09.166.

[6] P. Cardona *et al.*, "Modeling and operation strategy approaches for on-site Hydrogen Refuelling Stations," *International Journal of Hydrogen Energy*, vol. 52, pp. 49–64, 2024, doi: 10.1016/j.ijhydene.2023.08.192.

[7] S. Di Micco, M. Minutillo, A. Perna, and E. Jannelli, "On-site solar powered refueling stations for green hydrogen production and distribution: performances and costs," *E3S Web of Conferences*, vol. 334, 2022, doi: 10.1051/e3sconf/202233401005.

[8] M. A. Mahmood, P. Pérez de la Calle, J. M. Meneses Zuluaga, N. Massarotti, and C. Sanchez-Diaz, "Techno-economic evaluation of hydrogen refuelling station with on-site electrolysis production powered by photovoltaic solar energy for the railway sector," *International Journal of Hydrogen Energy*, vol. 138, no. February, pp. 802–822, 2025, doi: 10.1016/j.ijhydene.2025.05.094.

[9] D. Lanni, G. Di Cicco, M. Della Pietra, V. Cigolotti, and A. Perna, "Techno-Economic Assessment of Electrolytic Hydrogen Production for Refuelling Stations: Case Studies in Italy," *Proceedings - 24th EEEIC International Conference on Environment and Electrical Engineering and 8th I and CPS Industrial and Commercial Power Systems Europe, EEEIC/I and CPS Europe 2024*, pp. 1–6, 2024, doi: 10.1109/EEEIC/ICPSEurope61470.2024.10751144.

[10] S. Ren, X. Jia, S. Wang, P. He, S. Zhang, and X. Peng, "Creation and validation of a dynamic simulation method for the whole process of a hydrogen refueling station," *Journal of Energy Storage*, vol. 82, no. January, p. 110508, 2024, doi: 10.1016/j.est.2024.110508.

[11] M. Genovese and P. Fragiacomo, "Hydrogen refueling station: Overview of the technological status and research enhancement," *Journal of Energy Storage*, vol. 61, no. November 2022, p. 106758, 2023, doi: 10.1016/j.est.2023.106758.

[12] D. Apostolou and G. Xydis, "A literature review on hydrogen refuelling stations and infrastructure. Current status and future prospects," *Renewable and Sustainable Energy Reviews*, vol. 113, no. May 2018, 2019, doi: 10.1016/j.rser.2019.109292.

[13] J. Li *et al.*, "Optimal Investment of Electrolyzers and Seasonal Storages in Hydrogen Supply Chains Incorporated with Renewable Electric Networks," *IEEE Transactions on Sustainable Energy*, vol. 11, no. 3, pp. 1773–1784, 2020, doi: 10.1109/TSTE.2019.2940604.

[14] F. Grüger, O. Hoch, J. Hartmann, M. Robinius, and D. Stolten, "Optimized electrolyzer operation: Employing forecasts of wind energy availability, hydrogen demand, and electricity prices," *International Journal of Hydrogen Energy*, vol. 4, pp. 4387–4397, 2019, doi: 10.1016/j.ijhydene.2018.07.165.

[15] J. Kurtz, T. Bradley, E. Winkler, and C. Gearhart, "Predicting demand for hydrogen station fueling," *International Journal of Hydrogen Energy*, vol. 45, no. 56, pp. 32298–32310, 2020, doi: 10.1016/j.ijhydene.2019.10.014.

[16] H2 Mobility, "70MPa Hydrogen Refuelling Station Standardization - Functional Description of Station Modules," p. 27, 2010, [Online]. Available: https://www.now-gmbh.de/content/service/3-publikationen/1-nip-wasserstoff-und-brennstoffzellentechnologie/h2mobility_hrs_functional_description.pdf

[17] M. Minutillo, A. Cappiello, F. Romano, S. Di Micco, and G. Di Ilio, "Analysis of Hydrogen Demand and Refueling Infrastructure in the Road Transportation Sector in Europe," *Proceedings - 24th EEEIC International Conference on Environment and Electrical Engineering and 8th I and CPS Industrial and Commercial Power Systems Europe, EEEIC/I and CPS Europe 2024*, pp. 1–6, 2024, doi: 10.1109/EEEIC/ICPSEurope61470.2024.10751071.

[18] NIST, "NIST Standard Reference Database." https://webbook.nist.gov/chemistry/ (accessed Jun. 02, 2025).

[19] Impulsora Industrial Guadalajara S.A. de C.V., "TL apps - CATÀLOGO," 2021.

[20] D. Lanni, M. Minutillo, V. Cigolotti, and A. Perna, "Biomethane production through the power to gas concept: A strategy for increasing the renewable sources exploitation and promoting the green energy transition," *Energy Conversion and Management*, vol. 293, no. August, p. 117538, 2023, doi:

10.1016/j.enconman.2023.117538.
[21] D. Lanni, G. Di Cicco, M. Minutillo, V. Cigolotti, and A. Perna, “Techno-economic assessment of a green liquid hydrogen supply chain for ship refueling,” *International Journal of Hydrogen Energy*, vol. 97, no. November 2024, pp. 104–116, 2025, doi: 10.1016/j.ijhydene.2024.11.410.
[22] A. Elgowainy, K. Reddi, D. Y. Lee, N. Rustagi, and E. Gupta, “Techno-economic and thermodynamic analysis of pre-cooling systems at gaseous hydrogen refueling stations,” *International Journal of Hydrogen Energy*, vol. 42, no. 49, pp. 29067–29079, 2017, doi: 10.1016/j.ijhydene.2017.09.087.